Biomaterials 31 (2010) 1420–1428

Contents lists available at ScienceDirect

Biomaterials

journal homepage: www.elsevier.com/locate/biomaterials

The induction of tumor apoptosis in B16 melanoma following STAT3 siRNA delivery with a lipid-substituted polyethylenimine

Aws Alshamsan [a], Samar Hamdy [a], John Samuel [a,1], Ayman O.S. El-Kadi [a], Afsaneh Lavasanifar [a,b,**], Hasan Uludağ [a,b,c,*]

[a] Faculty of Pharmacy and Pharmaceutical Sciences, University of Alberta, USA
[b] Department of Chemical and Material Engineering, Faculty of Engineering, University of Alberta, USA
[c] Department of Biomedical Engineering, Faculty of Medicine and Dentistry, University of Alberta, USA

ARTICLE INFO

Article history:
Received 16 September 2009
Accepted 2 November 2009
Available online 13 November 2009

Keywords:
siRNA
STAT3
Melanoma
Cancer therapy
Polyethylenimine
Nanomedicine

ABSTRACT

Persistent activation of signal transducer and activator of transcription 3 (STAT3) has been shown to impart several oncogenic features in many solid and blood tumors. In this study, we investigated the potential of nanoparticles based on polyethylenimine (PEI) modified with stearic acid (StA), to deliver siRNA for efficient STAT3 downregulation in B16 melanoma cells. The B16 cells were targeted with ~6–200 nM of siRNA complexes for 36 h. Compared to the PEI complexes, the PEI-StA complexes showed higher potency in STAT3 silencing in B16 cells accompanied by a significant induction of IL-6 secretion and a reduction of VEGF production. Moreover, with PEI-StA complexes, the level of the cellular Caspase 3 activity (an indicator of apoptotic activity) was found to be 2.5 times higher than that of PEI complexes. When the cells were treated with 50 nM of siRNA complexes on a daily basis, the cell viability was dramatically reduced reaching only to 16% after the third daily dose of PEI-StA complexes, as compared to the 69% viability observed with the PEI complexes at an equivalent time period. Consistently, *in vivo* results indicated significant regression in tumor growth and tumor weight after siRNA/PEI-StA treatment as compared to the siRNA/PEI. This was accompanied with significant increase in IL-6 levels and Caspase 3 activity, and a significant decrease in VEGF level and STAT3 activity in the tumor tissue. The lipid-modified PEI is a promising carrier for siRNA delivery and downregulation of STAT3 by polymer-mediated siRNA delivery is an effective strategy for cancer treatment especially when an optimum delivery system can potentiate the silencing activity of siRNA.

1. Introduction

Persistent activation of signal transducer and activator of transcription 3 (STAT3) has been associated with malignant properties including tumor survival, proliferation, angiogenesis, and immune evasion in a vast number of solid and blood tumors [1]. STAT3 is a downstream protein that becomes activated by phosphorylation of a single tyrosine (Y^{705}) in response to cytokine and growth factor receptor stimulations [2]. The persistent activation of STAT3 is associated with persistent activation of tyrosine kinases including Src kinases, growth factor receptors with intrinsic kinase activity, and Janus kinases (JAKs) [3]. Upon activation, STAT3 dimerizes through reciprocal phosphotyrosine-SH2 interaction. The formed dimers translocate to the nucleus and bind to STAT-specific sites on the promoters of target genes to induce the transcription of proteins that have critical roles in regulating cell survival and proliferation (e.g. c-Myc, cyclin D1, and Bcl-family proteins) [2]. Hyperactivity of STAT3 in a large percentage of cells in different tumor types, its involvement in various malignant behaviors, and dependence of tumor cells on STAT3 for survival more than normal cells, make this molecule an attractive target for cancer therapy [4,5].

Inhibition of STAT3 signaling pathway has been achieved by several small molecules through either upstream inhibition of cytokine and growth factors [6,7], inhibition of STAT3 dimerization [8], inhibition of STAT3/STAT3 nuclear translocation [9] or inhibition of DNA binding activity [10]. However, cytotoxicity and lack of specificity has diminished the enthusiasm for pharmacological inhibitors of STAT3 and limited their progress from bench to bed

* Corresponding author. #526 Chemical and Materials Engineering Building, University of Alberta, Edmonton, AB, Canada T6G 2G6. Tel.: +1 780 492 0988; fax: +1 780 492 2881.
** Corresponding author. # 4119 Dent/Pharm Centre, University of Alberta, Edmonton, AB, Canada T6G 2N8. Tel.: +1 780 492 2742; fax: +1 780 492 1217.
E-mail addresses: alavasanifar@pharmacy.ualberta.ca (A. Lavasanifar), hasan.uludag@ualberta.ca (H. Uludağ).
[1] This manuscript is dedicated to the memory of Dr. John Samuel who initiated a research program encompassing the present study.

0142-9612/$ – see front matter © 2009 Elsevier Ltd. All rights reserved.
doi:10.1016/j.biomaterials.2009.11.003

side. In this context, application of small interfering RNA (siRNA) is an attractive alternative with a promising therapeutic potential for the inhibition of STAT3 in cancer [11,12].

The siRNA delivery has been shown to be effective in down-regulating STAT3 expression in several tumor cells. For instance, transfection of Hep2 laryngeal cancer cell line with DNA plasmid encoding for anti-STAT3 siRNA using Oligofectamine™, was shown to be successful in inhibition of STAT3 gene expression leading to the suppression of growth and induction of apoptosis in Hep2 cancer cell line [13]. Another study has reported that the delivery of siRNA by Lipofectamine™ 2000 for STAT3 silencing can induce apoptosis in astrocytoma cells [14]. The use of such carriers; however, is limited to *in vitro* studies due to high dose of siRNA needed to achieve STAT3 inhibition and possibility for the emergence of carrier-associated toxicity upon *in vivo* administration [15]. In order to achieve efficient RNA interference (RNAi)-based therapeutics, developing safe but efficient delivery system for siRNA remains a major priority.

An ideal siRNA delivery system for siRNA delivery in biological system should maintain siRNA stability under physiological conditions, improve its pharmacokinetics and biodistribution, and enhance siRNA potency while reducing potential off-target effects of siRNA [16]. Polymeric carriers, in particular, are attractive for siRNA delivery since they are considered safer than viral vectors and also more amenable for optimal design via chemical modification techniques when compared to viral or lipid based non-viral carriers [17–20]. The polymeric carrier polyethylenimine (PEI) is a preferred carrier for intracellular delivery of siRNA. Because of its high cationic charge density, PEI possesses the ability to effectively condense nucleic acids by electrostatic interaction between the anionic phosphates in the siRNA backbone and the cationic amines in the polymer [21]. It demonstrated effective siRNA delivery *in vitro* and *in vivo* to several cell types including cancerous cells (reviewed in [22]). The work of Urban-Klein et. al. signified the therapeutic applicability of PEI as a delivery system for siRNA-based cancer therapy [23]. Using siRNA targeting c-erbB2/neu (HER2) receptor, the authors demonstrated marked reduction in tumor growth following systemic (intraperitonial, i.p.) administration of the PEI/siRNA complex to mice bearing subcutaneous ovarian carcinoma xenograft [23]. The siRNA carrier used in this study was a linear low-molecular-weight PEI, which required a high polymer level (high N/P ratio) to achieve the desired complexation with siRNA. Application of a linear low-molecular-weight PEI with a low cationic charge density also led to the formation of larger particles upon nucleic acid compaction and showed lower transfection efficiency compared to branched PEI [24]. Overall, branched PEI (25 kDa) is a more effective system for nucleic acid delivery than its linear counterpart owing to higher complexation ability, smaller size of its particles and better interaction with cells [25].

We have recently developed improved polymeric systems for siRNA delivery to B16 melanoma cells, which were based on stearic acid (StA) derivatives of branched PEI. Modification of branched PEI with lipids led to better protection of siRNA integrity in biological milieu and also improved the siRNA delivery into the cytoplasm of cells [26]. As a result, enhanced silencing was obtained when the StA-derivative was used to deliver siRNA against α_v integrin. The latter served as a model target for demonstrating the feasibility of silencing and our previous studies were restricted to an *in vitro* culture system. In this study, we further evaluated the StA-substituted PEI carrier for siRNA-mediated downregulation of STAT3 in B16 melanoma cells, since recent data suggested that STAT3 was directly required for the initiation and promotion of mouse skin tumorigenesis [27]. The molecular and cellular consequences of such a STAT3 inhibition in tumor cells were determined based on identified targets (IL6 and VEGF secretion) and the studies were extended to a B16 tumor model in order to explore the effectiveness of the proposed carrier *in vivo* for the first time.

2. Materials and methods

2.1. Materials

Branched PEI (25 kDa), triethylamine (TEA), 3-(4,5-dimethylthiazol-2-yl)-2,5-diphenyltetrazolium bromide (MTT), dimethyl sulfoxide (DMSO), and stearoyl chloride (98.5%) were obtained from Sigma–Aldrich (St. Louis, MO). Anhydrous ethyl ether and dichloromethane (DCM) were purchased from Fisher Scientific (Fairlawn, NJ). Fetal Bovine Serum (FBS) was obtained from HyClone (Logan, UT). Dulbecco's Modified Eagle's Medium (DMEM), L-glutamine, and gentamicin were purchased from Gibco-BRL (Burlington, ON, Canada). Mouse IL-6 ELISA kit was purchased from e-Biosciences (San Diego, CA). Mouse VEGF Quantikine ELISA Kit was purchased from R&D Systems (Minneapolis, MN). Sequence-specific siRNA targeting murine STAT3 mRNA was purchased from Ambion (Austin, TX) (sense: 5′-GGACGACUUU-GAUUUCAACtt-3′, anti-sense: 5′-GUUGAAAUCAAAGUCGUCCtg-3′). The scrambled siRNAs Silencer® Negative Control #1 siRNA (Catalogue #AM4635) and Silencer® FAM™ labeled Negative Control #1 siRNA (Catalogue #AM4620), both purchased from Ambion (Austin, TX). Caspase 3 Assay Kit, Etoposide, Nonidet P-40, Protease Inhibitor Cocktails, and 4-Nitrophenyl phosphate were purchased Sigma–Aldrich (St. Louis, MO). SK-MEL-28 + IFN-γ Cell Lysate, anti-phosphotyrosine (Y^{705}) STAT3 monoclonal antibody, and anti-actin antibody (I-19) were purchased from Santa Cruz Biotechnology (Stanta Cruz. CA). ECL Plus™ detection kit was purchased from GE Healthcare Life Sciences (Piscataway, NJ).

2.2. Cells and animals

Murine B16.F10 cells were grown and propagated in DMEM supplemented with 10% FBS at 37 °C. Male C57Bl/6 mice were purchased from the Jackson Laboratory (Bar Harbor, ME, USA). All experiments were performed in accordance with the University of Alberta guidelines for the care and use of laboratory animals. All experiments were performed using 4–6 week old male mice.

2.3. Preparation and characterization of siRNA complexes

As previously described, PEI-StA was prepared by *N*-acylation of PEI with stearoyl chloride and characterized as described in [28]. Thereafter, complexes of desired siRNA concentrations were prepared as previously described in [26]. Particle sizes were determined by employing dynamic light scattering methodology and ζ-potentials were determined in water for each siRNA complex in water by 3 serial measurements using Zetasizer 3000 (Malvern, UK).

2.4. STAT3 knockdown by siRNA complexes

For STAT3 targeting, siRNA complexes were prepared at final siRNA concentrations of 6.25, 12.5, 25, 50, 100 and 200 nM. Thereafter, in 24-well plates, 1×10^5 B16 melanoma cells were incubated with the designated complexes at 37 °C. 200 nM naked STAT3 siRNA and identical complexes of 200 nM of scrambled siRNA were used as controls. To remove uninternalized complexes, B16 medium was replaced after 8 h. Then, tumor supernatants were collected at 36 h and levels of IL-6 and VEGF were determined by ELISA. Moreover, cells were lysed and active phosphorylated stat3 (p-stat3) levels were detected by Western blot. Optical intensity of p-stat3 band was quantified and normalized to actin protein band using ImageJ software (W. Rasband (2005) National Institutes of Health, Bethesda, MD, http://rsb.info.nih.gov/ij). Simultaneously, cancer cell viability was determined by MTT assay following 36 h of incubation with identical siRNA complexes.

2.5. Western blot

Cells were collected and washed twice with ice-cold PBS, then lysed in a buffer containing 30 mM HEPES (pH 7.5), 2 mM Na_3VO_4, 25 mM NaF, 2 mM EGTA, 2% Nonidet P-40, 1:100 protease inhibitor cocktails, 0.5 mM DTT and 6.4 mg/mL phosphatase substrate 4-nitrophenyl phosphate. Cell lysates were centrifuged for 20 s at 16,000×*g*. Total protein extract was determined by Micro BCA Protein Assay. Equal amounts of protein (20 μg) were loaded on 8% SDS-PAGE gel. Proteins were then transferred into PVDF membrane and were probed with anti-phosphotyrosine (Y^{705}) STAT3 monoclonal antibody. Stripped membranes were probed with anti-actin antibody (I-19). Membranes were developed using ECL Plus™ detection kit.

2.6. MTT assay

B16 cells, grown in 96-well flat-bottomed microplates, were treated as indicated. Thereafter, 100 μL of MTT solution in culture medium (0.5 mg/mL) was added to each well for 2 h. The formed formazan crystals were dissolved by adding 200 μL

of DMSO to each well. Optical density was measured at 550 nm using a microplate reader (Powerwave with KC Junior software; Bio-Tek, Winooski, VT). The results were converted into % viability relative to untreated sample. In another study, B16 cells in 96-well plates were challenged with a daily dose of 50 nM siRNA PEI and PEI-StA complexes for 3 consecutive days. Media was refreshed 8 h after each incubation to remove uninternalized complexes and MTT assay was carried out for 5 days from the first dose to assess cellular viability. Media was refreshed every day in all groups during this experiment.

2.7. Caspase 3 activity study

The Caspase 3 activity was measured as an indicator for apoptosis. For that purpose, B16 cells were treated with 50 nM siRNA in PEI or PEI-StA for 24 h. Using Caspase 3 Assay Kit, cells were normalized for 10^5 cells per treatment group, lysed, and placed in designated wells in 96-well flat-bottomed microplates. Provided Caspase 3 inhibitor (Ac-DEVD-CHO) and Caspase 3 substrate (Ac-DEVD-pNA) were then added to designated wells according to the manufacturer's instructions. Optical density was measured at 405 nm using microplate reader and Caspase 3 activity was calculated based on *p*-Nitroaniline calibration curve.

2.8. STAT3 silencing in vivo

For tumor establishment, 0.75×10^6 B16 cells were inoculated subcutaneously in the upper left flank of male C57Bl/6 mice. After 10 days, 500 pmol of STAT3 targeting or scrambled siRNAs complexes in normal saline were administered to randomly-assigned groups (5 mice per group) by intratumoral injections on daily basis for 4 days. Untreated control group received daily intratumoral injections of normal saline. Tumor dimensions were measured by vernier caliper once a day during treatment period. The longest length and the perpendicular shorter length were multiplied to obtain tumor area (mm^2). Thereafter, mice were euthanized 1 day after the final treatment dose and tumor samples were immediately isolated and weighed. Consequently, isolated tumors were crushed between two slides to form uniform cell suspension. Tumor supernatants were obtained after centrifugation and normalized protein content was analyzed for IL-6 and VEGF using corresponding ELISAs as previously described. Cellular part was lysed and analyzed for STAT3 activation and Caspase 3 activity as described above.

2.9. Data analysis

IC_{50} for STAT3 knockdown was calculated using four parameter logistic function (SigmaPlot for Windows, Version 10.0). The data were analyzed for statistical significance ($p < 0.05$) by one-way ANOVA; Post-Hoc Scheffé's test was conducted to determine level of significance (SPSS for Windows, Version 16.0).

3. Results

3.1. Characterization of siRNA complexes

The average hydrodynamic diameter and ζ-potential of the siRNA complexes with PEI and PEI-StA are summarized in Fig. 1. Both complexes formed ~110 nm structures with no significant differences in diameter. The complexes displayed positive net surface charge, where the complexes with the unmodified PEI showed 4.9-fold higher ζ-potential value than the PEI-StA complexes.

3.2. STAT3 knockdown by siRNA complexes

To evaluate the ability of complexes for STAT3 knockdown, B16 melanoma cells were targeted with siRNA doses ranging from 6.25 to 200 nM. The knockdown of the active protein, p-stat3, was dependant on the siRNA dose (Fig. 2a). Levels of p-stat3 after incubation with PEI-StA complex were found to be 55.8% lower than that of PEI at 50 nM siRNA. At 100 nM siRNA, PEI-StA complexes also showed up to 42.2% reduction in p-stat3 levels compared to the PEI complexes. At 200 nM siRNA, there was no significant difference between the two polymers in spite of further p-stat3 reduction. It is worth noting that 25 nM siRNA was sufficient for PEI-StA complex to reach significant reduction in p-stat3 level. The observed knockdown is considered specific since 200 nM of scrambled siRNA did not show any significant reduction in p-stat3 levels (not shown). The IC_{50} of STAT3 knockdown was calculated based on the data in Fig. 2a. PEI-StA complexes had an IC_{50} value of 19.0 ± 3.0 nM for p-stat3 knockdown, significantly lower than that of PEI complexes (94.3 ± 23.7 nM; $p < 0.05$).

3.3. Effect of STAT3 knockdown on B16 survival in vitro

To examine B16 cells survival following STAT3 knockdown, we measured cell viability using the MTT assay. After 36 h of incubation

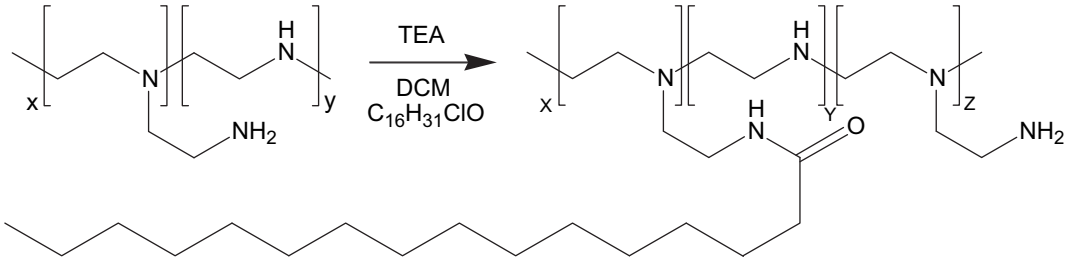

Polymer	Diameter (nm)	ζ Potential (mV)
PEI	112 ± 21	34.3 ± 4.5
PEI-StA	110 ± 2	5.8 ± 1.2

Fig. 1. Fatty acid attachment on PEI backbone and characteristics of the siRNA complexes. Table represents the size and zeta potential of siRNA complexes in averages of 3 different measurements (±SD).

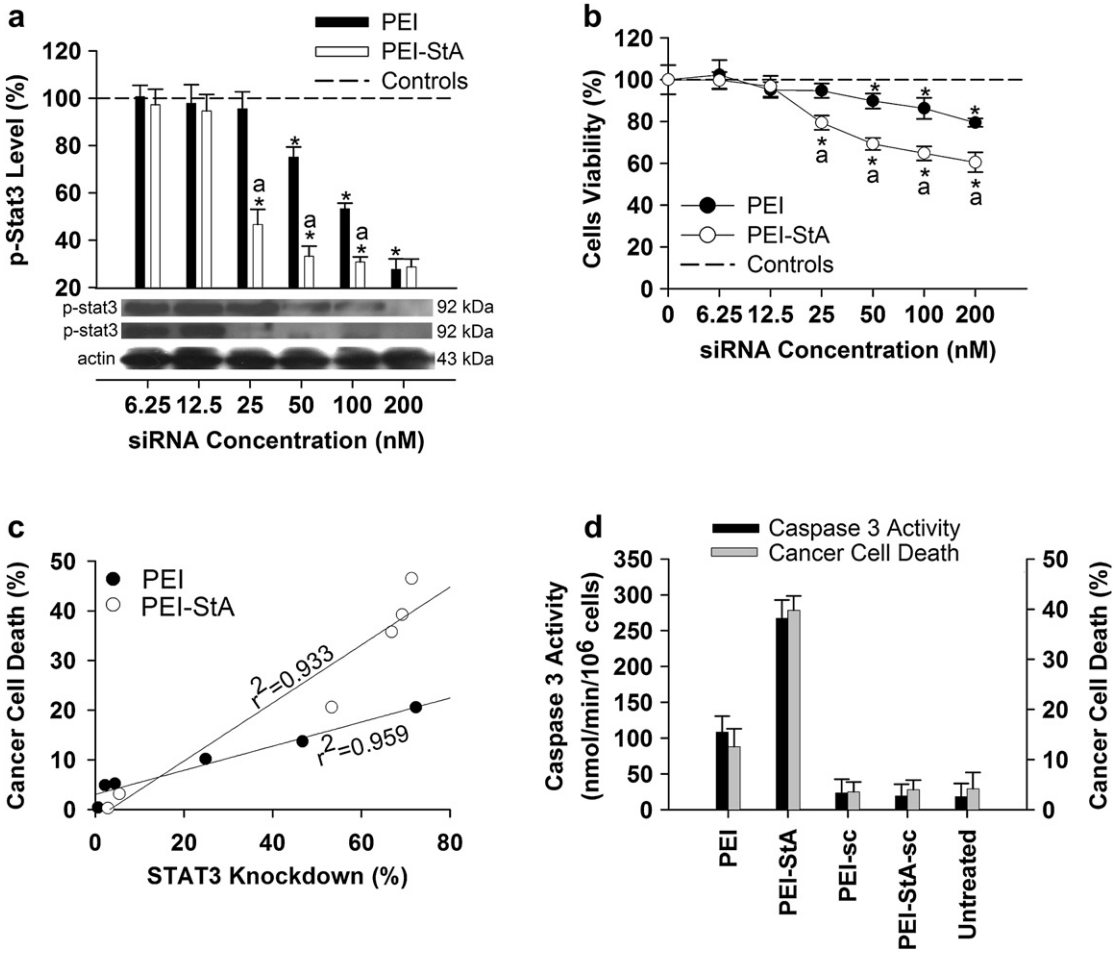

Fig. 2. STAT3 knockdown by siRNA complexes *in vitro*. (a) Western blot analysis showing a dose-dependent reduction in p-stat3 signal using actin as loading control. Bars represent expression of p-stat3 upon the designated siRNA treatment. Data are shown as the average ± SD of 4 experiments. (b) Percentage of cell viability was determined relative to untreated control by MTT assay. Data are shown as mean (±SD) of 7 replicates for each sample. (c) Correlation between p-stat3 knockdown and cancer cell death was determined by linear regression. Correlation co-efficient (r^2) for each set is expressed on the trend line of best fit. (d) Correlation between Caspase 3 activity (black bars) and cell death % (grey bars). PEI-StA caused higher apoptosis as compared to control (*; $p < 0.05$) and PEI (a; $p < 0.05$). Data are shown as mean (±SD) of 3 experiments. Where shown, dashed line represents controls including: 200 nM of naked siRNA or identical complexes of scrambled siRNA. Statistical significance was determined compared to control (*; $p < 0.05$) and PEI (a; $p < 0.05$).

with the complexes, a dose-dependent cytotoxicity was obtained with all complexes (Fig. 2b). At siRNA concentration of 50 nM, both complexes caused significant cytotoxicity of B16 melanoma cells, but cell viability was 18.5% lower after treatment with PEI-StA2 complexes as compared to that of PEI complexes. These results were consistent with the Western blot analysis. The possibility of non-specific cell death was tested using 200 nM of scrambled siRNA complexes and there were no significant changes in cell viability compared to untreated control. A strong correlation between the siRNA-mediated p-stat3 knockdown (data from Fig. 2a) and B16 cell death (data from Fig. 2b) was observed with all complexes, where the correlation coefficients (r^2) were 0.933 and 0.959 for PEI and PEI-StA complexes (Fig. 2c).

In order to confirm apoptosis, Caspase 3 activity was measured after treatment with 50 nM siRNA (Fig. 2d). While controls showed basal Caspase 3 activity, PEI complexes resulted in up to 6-fold increased Caspase 3 activities as compared to the untreated cells. When PEI-StA was used, Caspase 3 activity reached to 14.9 folds more than the untreated control. Consistent with our cytotoxicity results, Caspase 3 activity with the PEI-StA complexes was found to be ~2.5 times higher than that with PEI complexes. With formulations of scrambled siRNA using both polymers, no significant difference was noticed compared to untreated cells.

We then investigated the changes in cell viability after STAT3 silencing with fixed daily dose of siRNA (Fig. 3). The B16 cells were incubated with 50 nM fresh siRNA complexes of PEI or PEI-StA every 24 h for 3 consecutive days, and cell viability was measured for 7 days. After 24 h, PEI-StA complexes caused 39.7% decrease in cancer cell viability, which was statistically better than what achieved by PEI complexes (12.6% reduction in cell viability). The second dose allowed for dramatic reduction in cell viability where PEI-StA complexes caused 73.9% decrease in cell viability as compared to only 23.9% reduction caused by PEI complexes. A third dose of PEI complexes further reduced cell viability by 30.6%, but with PEI-StA complexes reduction in cell viability was remarkably more reaching over 84.7% cell death. After treatment removal, cells started to regain viability and continued to grow back. A similar study was carried out with identical formulations of scrambled siRNA where no significant changes in cancer cell viability were noticed.

3.4. *In vitro cytokine secretion by B16 cells*

To examine changes in the cytokine profile of B16 cells following STAT3 knockdown, B16 supernatants were collected after designated treatments and analyzed for IL-6 and VEGF. At 36 h after incubation, there was an increase in IL-6 secretion as a function of

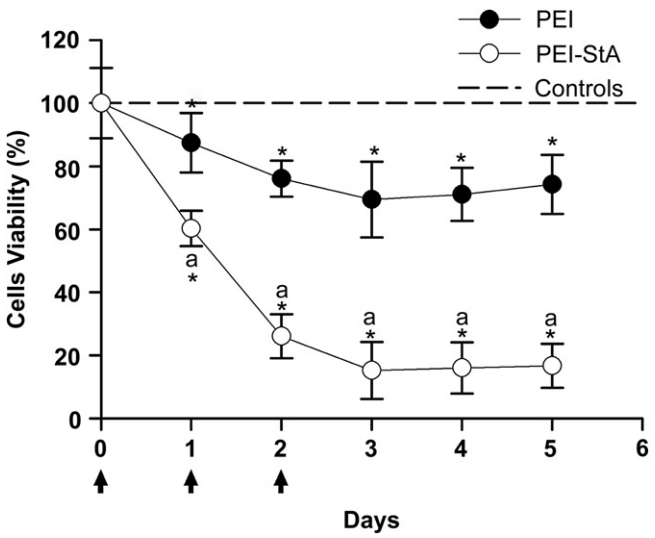

Fig. 3. Effect of multiple administration of 50 nM siRNA complexes on B16 viability *in vitro*. B16 cell viability is dramatically reduced by daily supplementation of anti-STAT3 siRNA in PEI and PEI-StA complexes. PEI-StA gave higher cell death as compared to control (*; $p < 0.05$) and PEI (a; $p < 0.05$). Data are shown as the average (±SD) of 3 independent experiments.

siRNA concentration used for STAT3 knockdown (Fig. 4a). Unlike the PEI complexes, PEI-StA complexes mediated a significant increase in IL-6 levels at 25 nM siRNA. At this concentration, p-stat3 level was also significantly lower compared to the PEI complexes. Both polymers showed significant increase in IL-6 secretion at 50 nM siRNA; however, IL-6 concentration after treatment with PEI-StA complexes was 42.7% higher than the PEI complexes. Further increase in IL-6 levels was observed at 100 nM, where PEI-StA complexes produced higher IL-6 levels (33.4% higher than that of PEI complexes). The IL-6 concentration reached plateau at 200 nM with both polymers.

A dose-dependent decrease in VEGF concentration in B16 supernatant was observed following 36 h of siRNA treatment (Fig. 4b). Consistent with the previous Western blot data, a significant reduction in VEGF level was detected at 25 nM siRNA with the PEI-StA complexes, but not with PEI complexes. Although all complexes significantly reduced VEGF secretion at 50 nM, PEI-StA mediated a higher reduction in VEGF level compared to PEI complexes. A more profound reduction in VEGF concentration was detected at 100 nM siRNA, where PEI-StA accounted for 27.2% decrease in measured VEGF concentration compared to the PEI complexes.

3.5. Effect of STAT3 knockdown on B16 tumor in vivo

To assess changes in tumor area after siRNA silencing of STAT3, we administered siRNA complexes intratumorally to an already established B16 tumor model. The results showed significant retardation in tumor growth after 4 days of administration of STAT3 siRNA by PEI-StA as compared to PEI (Fig. 5a). Scrambled siRNA complexes did not show any significant difference from untreated control at any point throughout the study. By the end of the study, tumor area for animals treated by PEI-StA/siRNA complexes was 2-fold smaller than those treated with PEI/siRNA complexes (Fig. 5a). Comparing the weights of isolated tumors, only STAT3-specific siRNA complexes showed significant reduction in tumor weight as compared to the controls (Fig. 5b). Nevertheless, siRNA delivery with the PEI-StA showed a 38% reduction in tumor weight as compared to the delivery with PEI. A superior antitumor effect of

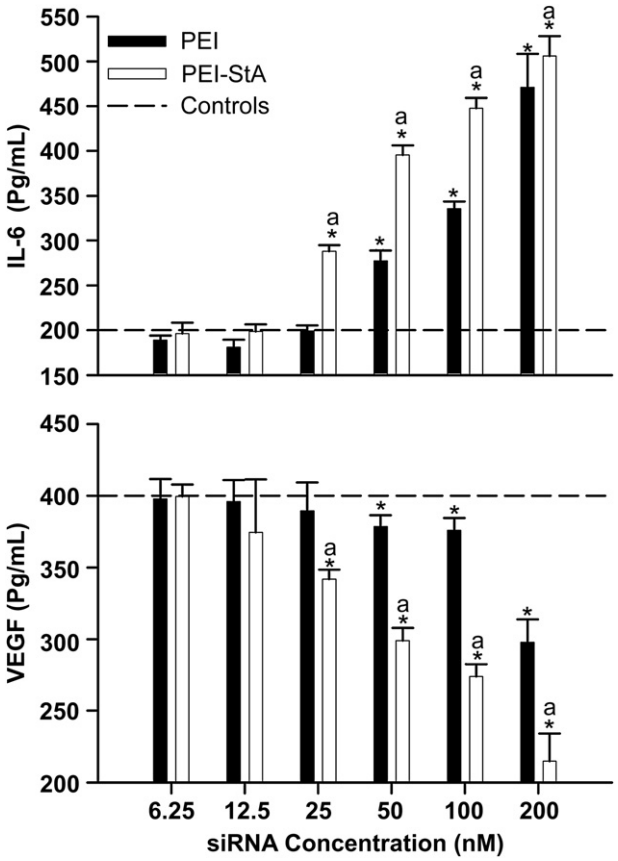

Fig. 4. Analysis of cytokine profile after STAT3 knockdown *in vitro*. Cytokine levels measured by ELISA were plotted in bar graphs for IL-6 (top) and VEGF (bottom) where PEI-StA showed significant induction of IL-6 production and decrease in VEGF levels as compared to control (*; $p < 0.05$) and PEI (a; $p < 0.05$). Dashed line represents controls which include 200 nM of naked siRNA or identical complexes of scrambled siRNA. Data are shown as the average (±SD) of 3 measurements.

STAT3-specific PEI-StA complexes over PEI and other controls was also evident visually at the time of sacrifices (Fig. 5c).

The western blot analysis of tumor homogenates showed that PEI-StA complexes were able to successfully reduce p-stat3 levels by ~41% and 60% lower than what achieved by PEI complexes and untreated control, respectively (Fig. 6a). This significant inhibition in p-stat3 was accompanied by a significant increase in Caspase 3 activity in PEI-StA treated groups, which was 2-fold and 22-fold higher than the PEI complex treated and the untreated control groups, respectively (Fig. 6b). In agreement with the *in vitro* data, IL-6 level was significantly higher in PEI-StA/siRNA treated tumors, with 2-fold and 6-fold increase as compared to the PEI/siRNA treatment and the untreated control groups, respectively (Fig. 6c). Consistently, VEGF level after PEI-StA/siRNA treatment was 3-fold and 5-fold less than the PEI/siRNA treatment and the untreated control groups, respectively (Fig. 6d).

4. Discussion

The first direct evidence suggesting a critical role of STAT3 in cancer growth emerged when it was shown that downregulation of STAT3 in cell lines derived from patients with squamous cell carcinoma of the head and neck (SCCHN) reduced the proliferation of SCCHN cells [29]. Subsequent studies revealed that STAT3 is also persistently activated in other solid and hematological malignancies in human [30,31], and plays an important role in tumor growth and progression (reviewed in [5,32]). Interruption of the STAT3

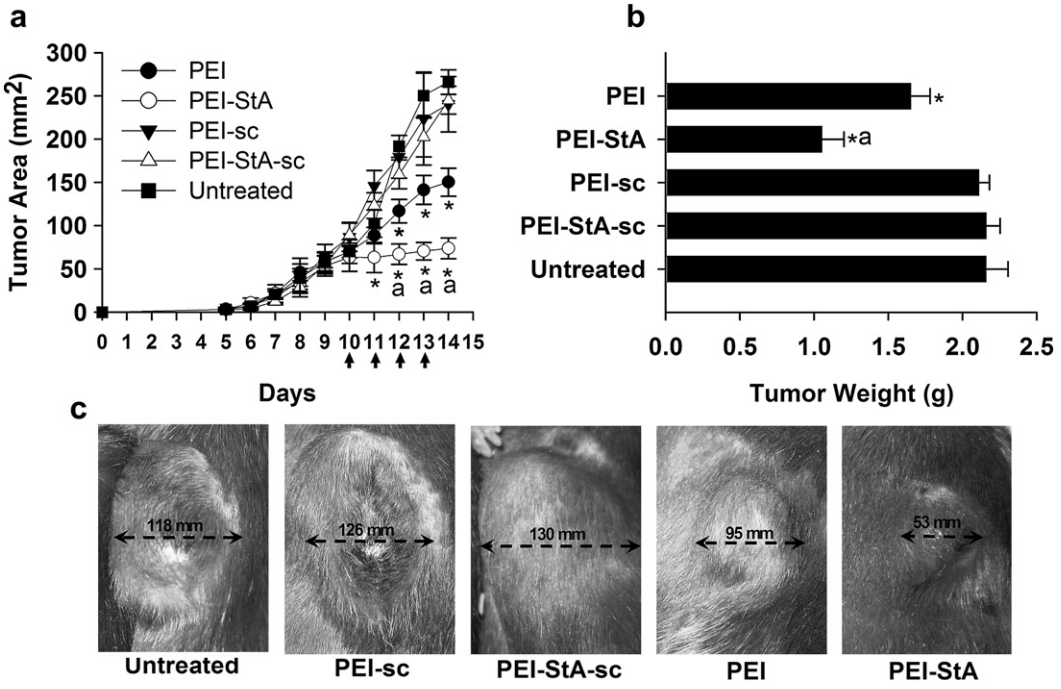

Fig. 5. Effect of siRNA complexes on tumor growth *in vivo*. (a) Male C57Bl/6 mice (5 per group) with established B16 tumors were injected with 500 pmol siRNA complexes for 4 days intratumorally. Tumor size was measured daily. The mean tumor area (±SEM) for each group was plotted versus time. PEI-StA shows higher retardation in tumor growth as compared to control (*; $p < 0.05$) and PEI (a; $p < 0.05$). (b) Tumor weight was measured at the endpoint of the study. Bars represent mean weight (±SEM) of the isolated tumors from each group. (c) Pictures representative for mice in each group at the endpoint of the study.

signaling pathway in solid and hematological tumors were proposed to serve as a promising strategy for cancer therapy [33]. For instance, in a study where both JAK and STAT3 were inhibited, a reduced tumor invasion and an increased apoptosis were noted in a human colorectal cancer model [34]. Additionally, in a phase I/II clinical trial, tipifarnib (a farnesyl transferase inhibitor) was administered to patients with breast cancer in combination with doxorubicin and cyclophosphamide [35]. The authors found that p-STAT3 was inhibited in patients upon tipifarnib treatment, which produced higher pathologic complete response rate than chemotherapy alone.

Several modalities have been employed to achieve effective STAT3 inhibition [11,33]. Peptides and peptideomimetics were introduced as inhibitors of STAT3 dimerization [8], but the effectiveness of these molecules was limited by the poor cellular permeability and insufficient stability profile. Small molecular inhibitors of STAT3 such as JSI-124 (cucurbitacin I) were shown to induce cell death and inhibit cell growth of transformed murine fibroblasts and human breast cancer [6]. However, non-specific toxicity limited the clinical application of JSI-124. At effective JAK2/STAT3 inhibitory concentration, JSI-124 was shown to profoundly affect actin cytoskeleton via STAT3-independend mechanism in both cancerous and non-cancerous cells [36]. More tolerable natural agents such as curcumin reported to exert STAT3 inhibitory action in cancer [10,37], required high concentrations to excerpt this effect (40–50 μM), raising concerns for its potential non-specific effects. A Phase II clinical trial investigating the anti-cancer potential of curcumin in prostate cancer patients indicated low bioavailability of curcumin when administered orally [38].

RNA interference has been examined for STAT3 inhibition in cancer as a more specific modality. However, the therapeutic potential of siRNA is hindered by its poor cellular internalization and biological instability [39]. Development of efficient and safe delivery systems that can correct these properties of siRNA will be paramount for its clinical application. Numerous non-viral carriers have been investigated for siRNA delivery, such as PEI, cationic liposomes, polyelectrolyte complex micelles, water soluble lipopolymers, and polycationic dendrimers. The knockdown of STAT3 by siRNA inducing apoptosis in astrocytoma cell lines has been achieved by high siRNA doses (20–60 μM) using Oligofectamine™ as carrier [14]. Moreover, STAT3 knockdown by siRNA at 100 nM using Lipofectamine™ 2000 was shown to induce apoptosis and limit invasiveness and motility of human prostate cancer cells *in vitro* [40]. High siRNA doses used in such studies raise the concern for off-target effects. Besides, application of mentioned carriers has been associated with cellular toxicity limiting their *in vivo* use [15]. In this manuscript, we report on a potent siRNA polyplex that achieved efficient downregulation of STAT3 at a relatively low siRNA concentration (~25 nM) (Fig. 2a) and inhibited tumor growth both *in vitro* (Fig. 2b) and *in vivo* (Fig. 6a). This polyplex was based on StA attachment to branched PEI (25 kDa) (Fig. 1), which was recently reported to form complexes with siRNA, interact with B16 melanoma cells *in vitro* and reduce the expression of α_v integrin in those cells [26]. We evaluated this system for STAT3 targeting as a cancer therapeutic modality *in vitro* and *in vivo*. The dependence of B16 melanoma cells on STAT3 activity for their survival has been previously established [41].

Our findings demonstrate that PEI and PEI-StA polymers both effectively pack siRNA into polyelectrolyte complexes suitable for cell internalization. However, cellular association of siRNA is higher when packed by PEI-StA as compared to PEI (not shown). The higher degree of siRNA protection in serum by PEI-StA might have contributed to this effect [26]. Others have also shown that better siRNA protection from serum degradation by its delivery system to be correlated with a higher cellular association of complexed siRNA [42,43].

The improved association of siRNA with cells, in turn, will lead to higher siRNA silencing efficacy [43]. In this study, both PEI and PEI-StA siRNA complexes were equipotent in STAT3 knockdown at 200 nM siRNA, but PEI-StA yielded significant silencing effect and

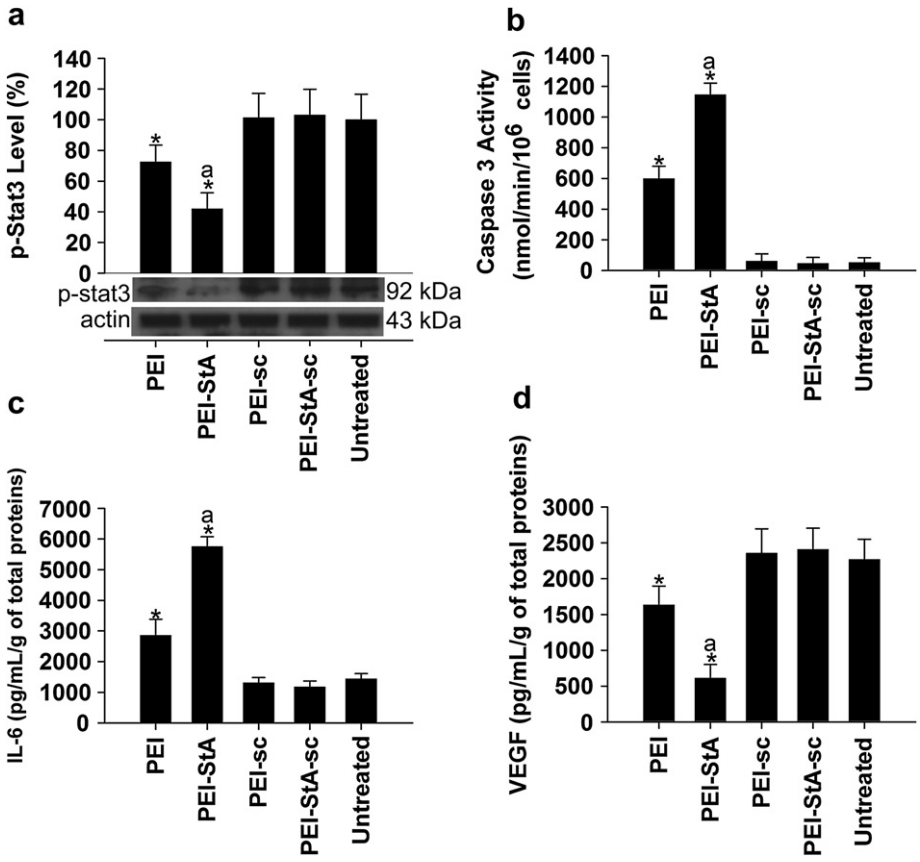

Fig. 6. Molecular analysis of tumor following siRNA administration *in vivo*. (a) p-STAT3 was detected in 20 μg of collected cell lysate from each treatment group by Western blot. Data are shown as the average (±SD) of 4 measurements. (b) Caspase 3 activity was measured in each treatment group. Data represent the mean of 6 measurements (±SD). (c) & (d) Levels of IL-6 and VEGF, respectively, in tumors from each treatment group as determined by ELISA. Data represent the mean (±SD) of at least 3 measurements. Significance levels are indicated by (*; $p < 0.05$) as compared to control and (a; $p < 0.05$) as compared to PEI.

enhanced cancerous cell death at siRNA concentrations as low as 25 nM (Fig. 2a). This is expected to be beneficial to reduce possible siRNA off-target effects as a consequence of the reduced dose. Secondly, lower polymer contents were needed for siRNA complexation when PEI-StA was used in comparison to PEI. Therefore, application of PEI-StA as the siRNA complexing agent may help to minimize potential inherent toxicity of PEI against non-target cells.

The *in vitro* STAT3 knockdown efficacy for both carriers was highly correlated with B16 cell death (Fig. 2c), with PEI-StA appearing to be a more efficient siRNA carrier than PEI in down regulating the expression of STAT3 and reducing growth of B16 cells (Fig. 2a and b). Interestingly, at similar STAT3 levels, PEI-StA complexes resulted in more cancer cell death than what was achieved with PEI complexes (Fig. 2c). This is most likely a result of more efficient delivery of siRNA by PEI-StA to its cellular and intracellular targets. Although non-specific toxicity of the polymers could complicate the interpretation of our results, the dose-dependent reduction in cancer cell viability observed in this study was unlikely to be due to non-specific polymer cytotoxicity, since; (i) the noted cell death after STAT3 knockdown by siRNA is shown to be an apoptotic rather than a necrotic event (Fig. 2d) (i.e., cytotoxic effect of polymers is usually mediated via necrosis) and (ii) at the highest siRNA concentration used in this study (i.e., highest polymeric amount), both PEI and PEI-StA were proven not to be toxic on B16 cells [26].

It is worth noting that 50% inhibition in cancer cell survival *in vitro* was only achieved by PEI-StA complex (and not with PEI complex) and just after daily administration of siRNA complexes (Fig. 3). The necessity for multiple dosing of siRNA complexes is not surprising because of the temporary nature of siRNA interference owing to its degradation by intracellular nucleases, which can be compensated by the daily supplementation of siRNA complexes. Such information was valuable in scheduling our *in vivo* study where daily administration of anti-STAT3 siRNA complexes for 4 days significantly suppressed tumor growth rate (Fig. 5a). Although no reduction in the originally treated tumor mass was noted, groups treated with PEI and in particular PEI-StA/STAT3 siRNA complexes, demonstrated remarkable inhibition in tumor growth and significant induction of apoptosis *in vivo* compared to scrambled siRNA complexes and untreated controls (Fig. 6b).

Upon STAT3 knockdown, an increase in IL-6 production and a decrease in VEGF production by B16 cells were detected *in vitro* (Fig. 4a and b) and *in vivo* (Fig. 6c and d). Consistent with previous findings of this paper, the reduction in STAT3 expression leading to increase in Caspase3 activity, increase in IL-6 production and decrease in VEGF secretion was more pronounced for PEI-StA/siRNA complexes than that of PEI. IL-6 is a pleiotropic cytokine with paradoxical effects. In some cases, IL-6 promotes tumor growth, while exerting anti-tumoral activity in other cases, and being used for the treatment of malignancies such as melanoma [44]. This paradox is partly due two opposing transcription factors activated by the IL-6 signaling, namely STAT3 and STAT1 [45]. In many cancer types, IL-6 constitutively activates STAT3, whereas STAT1 activation by IL-6 seems to be transient and inefficient especially when compared to its activation by interferon alpha (IFN-α) and

interferon gamma (IFN-γ) [46]. Interestingly, in the absence of STAT3, IL-6 causes a drastic and prolonged activation of STAT1, and induces the same spectrum of genes that are induced by IFN-γ with similar kinetics and response [47]. Such an effect would directly translate into suppression of B16 cell growth [48]. Therefore, we argue that one reason for the noted cancer regression after STAT3 knockdown in this study is perhaps the anti-tumoral effect of IL-6 that is reminiscent of the IFN-γ effect. Moreover, the expression of IL-6 is known to be induced by IFN-γ [49] and NFκB activity [50]. Upon IL-6 expression, STAT3 strongly inhibits IFN expression [51] and suppresses NFκB activity [52]. Therefore, when STAT3 is downregulated, it is logical to expect an induction in IL-6 production. Our results showed a dose-dependent increase in IL-6 secretion *in vitro* associated with STAT3 knockdown. Similarly, we detected an enhanced production of IL-6 in the isolated tumor tissue (Fig. 6c) where STAT3 is downregulated (Fig. 6a). An independent group has also reported similar observation where induction of IL-6 production was detected in B16 melanoma cells *in vivo* after STAT3 targeting by anti-sense oligonucleotide [53]. In contrast to our findings, another study reported a reduction of IL-6 mRNA in B16.F10 after interrupting STAT3 signaling [9]. The reason behind this discrepancy is unclear to us, but we note that the approach used by these authors to suppress STAT3 activity was by suppression of STAT3 nuclear translocation by decoy oligonucleotide with no inhibition of cytoplasmic levels of STAT3. The presence of STAT3 in the cytoplasm raises the possibility of STAT3 inhibition on NFκB [54]. Recently, it was suggested that STAT3 could interact with p65 subunit to form a novel complex that suppresses P-NFκB activity [55]. In our siRNA-based approach as well as in the anti-sense oligonucleotide approach [53], intracellular protein levels of STAT3 was reduced, which minimized the negative effect on NFκB and, hence, promoted the IL-6 production. However, because IL-6 is also produced *in vivo* by components of the immune systems, we cannot attribute all IL-6 secretion solely to tumor cells. A more detailed analysis of the infiltrating immune cells to the tumor mass and the possible anti-tumoral immune response is currently ongoing in our lab.

The reduction in the VEGF levels as a result of STAT3 knockdown was expected since VEGF gene expression was shown to be upregulated by STAT3 [56]. Beside its role for tumoral angiogenesis, the importance of VEGF for B16 survival has been demonstrated [57]. Considering the well established relationship between the VEGF expression, tumor vascularization and cancer survival, we expect the regression in tumor growth *in vivo* after STAT3 inhibition was due to both its direct effects on cancer cell survival and its anti-angiogenic effect on tumor tissue mass. However, we could not rule out the possibility of B16 cell death due to reduced expression of other antiapoptotic proteins as a result of STAT3 knockdown. It has been demonstrated that STAT3 upregulates the expression of several antiapoptotic proteins such as Bcl-2, Bcl-xL, and Mcl-1 [33] and the inhibition of STAT3 activity results in an increased sensitivity to apoptosis [58]. Moreover, the detrimental effects of STAT3 disruption on B16 survival has been linked to inhibition in Bcl-xL expression [58]. It will be important to elucidate the role of other intracellular proteins involved upon STAT3 inhibition, and this may identify better therapeutic targets.

5. Conclusion

To date, no strategy for STAT3 inhibition has reached clinical application as a cancer therapeutic. Although, RNAi technology carries promising efficacy for cancer treatment by STAT3 knockdown, the poor stability and cellular availability stands against siRNA therapeutic potentials. In this study, we developed a delivery system based on stearic acid modification of PEI, which turned to significantly increases siRNA potency *in vitro* and *in vivo* and consequently reduces off-target effects. Such approach harbors a promise for therapeutic applications for cancer that is still lacking in spite of the reported efficacy of siRNA for cancer treatment in experimental settings.

Acknowledgements

This project was funded by operating grants to J.S. and A.L. from the Canadian Institute of Health Research (MOP 42407) and to H.U. from CIHR (MOP 74452) and NSERC. A.A. is sponsored by an active scholarship from the Saudi Ministry of Higher Education. B16.F10 cell line was kindly provided by Dr. Mavanur Suresh, University of Alberta. Mrs. Vanessa Incani is highly thanked for synthesizing PEI-StA. Technical help of flow cytometry facility staff is acknowledged, Cross Cancer Institute, Edmonton, AB, Canada.

References

[1] Jing N, Tweardy DJ. Targeting Stat3 in cancer therapy. Anticancer Drugs 2005;16(6):601–7.
[2] Turkson J, Jove R. STAT proteins: novel molecular targets for cancer drug discovery. Oncogene 2000;19:6613–26.
[3] Buettner R, Mora LB, Jove R. Activated STAT signaling in human tumors provides novel molecular targets for therapeutic intervention. Clin Cancer Res 2002;8:945–54.
[4] Yu CL, Meyer DJ, Campbell GS, Larner AC, Carter-Su C, Schwartz J, et al. Enhanced DNA-binding activity of a Stat3-related protein in cells transformed by the Src oncoprotein. Science 1995;269(5220):81–3.
[5] Yu H, Jove R. The STATs of cancer–new molecular targets come of age. Nat Rev Cancer 2004;4(2):97–105.
[6] Blaskovich MA, Sun J, Cantor A, Turkson J, Jove R, Sebti SM. Discovery of JSI-124 (cucurbitacin I), a selective Janus kinase/signal transducer and activator of transcription 3 signaling pathway inhibitor with potent antitumor activity against human and murine cancer cells in mice. Cancer Res 2003;63(6):1270–9.
[7] Bharti AC, Donato N, Aggarwal BB. Curcumin (diferuloylmethane) inhibits constitutive and IL-6-inducible STAT3 phosphorylation in human multiple myeloma cells. J Immunol 2003;171(7):3863–71.
[8] Turkson J, Ryan D, Kim JS, Zhang Y, Chen Z, Haura E, et al. Phosphotyrosyl peptides block Stat3-mediated DNA binding activity, gene regulation, and cell transformation. J Biol Chem 2001;276(48):45443–55.
[9] Liu X, Li J, Zhang J. STAT3-decoy ODN inhibits cytokine autocrine of murine tumor cells. Cell Mol Immunol 2007;4(4):309–13.
[10] Deng J, Grande F, Neamati N. Small molecule inhibitors of Stat3 signaling pathway. Curr Cancer Drug Targets 2007;7(1):91–107.
[11] Yue P, Turkson J. Targeting STAT3 in cancer: how successful are we? Expert Opin Investig Drugs 2009;18(1):45–56.
[12] Cejka D, Losert D, Wacheck V. Short interfering RNA (siRNA): tool or therapeutic? Clin Sci (Lond) 2006;110(1):47–58.
[13] Gao LF, Xu DQ, Wen LJ, Zhang XY, Shao YT, Zhao XJ. Inhibition of STAT3 expression by siRNA suppresses growth and induces apoptosis in laryngeal cancer cells. Acta Pharmacol Sin 2005;26(3):377–83.
[14] Konnikova L, Kotecki M, Kruger MM, Cochran BH. Knockdown of STAT3 expression by RNAi induces apoptosis in astrocytoma cells. BMC Cancer 2003;3:23.
[15] Omidi Y, Hollins AJ, Benboubetra M, Drayton R, Benter IF, Akhtar S. Toxicogenomics of non-viral vectors for gene therapy: a microarray study of lipofectin- and oligofectamine-induced gene expression changes in human epithelial cells. J Drug Target 2003;11(6):311–23.
[16] Thomas M, Lu JJ, Chen J, Klibanov AM. Non-viral siRNA delivery to the lung. Adv Drug Deliv Rev 2007;59(2–3):124–33.
[17] Uprichard SL. The therapeutic potential of RNA interference. FEBS Lett 2005;579(26):5996–6007.
[18] Kennedy D. Breakthrough of the year. Science 2002;298(5602):2283.
[19] Behlke MA. Progress towards in vivo use of siRNAs. Mol Ther 2006;13(4):644–70.
[20] Putnam D, Doody A. RNA-interference effectors and their delivery. Crit Rev Ther Drug Carrier Syst 2006;23(2):137–64.
[21] Demeneix B, Behr JP. Polyethylenimine (PEI). Adv Genet 2005;53:217–30.
[22] Aigner A. Gene silencing through RNA interference (RNAi) in vivo: strategies based on the direct application of siRNAs. J Biotechnol 2006;124(1):12–25.
[23] Urban-Klein B, Werth S, Abuharbeid S, Czubayko F, Aigner A. RNAi-mediated gene-targeting through systemic application of polyethylenimine (PEI)-complexed siRNA in vivo. Gene Ther 2005;12(5):461–6.
[24] Lungwitz U, Breunig M, Blunk T, Gopferich A. Polyethylenimine-based non-viral gene delivery systems. Eur J Pharm Biopharm 2005;60(2):247–66.
[25] Godbey WT, Wu KK, Mikos AG. Size matters: molecular weight affects the efficiency of poly(ethylenimine) as a gene delivery vehicle. J Biomed Mater Res 1999;45(3):268–75.

[26] Alshamsan A, Haddadi A, Incani V, Samuel J, Lavasanifar A, Uludag H. Formulation and delivery of siRNA by oleic acid and stearic acid modified polyethylenimine. Mol Pharm 2009;6(1):121–33.
[27] Kataoka K, Kim DJ, Carbajal S, Clifford JL, DiGiovanni J. Stage-specific disruption of Stat3 demonstrates a direct requirement during both the initiation and promotion stages of mouse skin tumorigenesis. Carcinogenesis 2008;29(6):1108–14.
[28] Incani V, Tunis E, Clements BA, Olson C, Kucharski C, Lavasanifar A, et al. Palmitic acid substitution on cationic polymers for effective delivery of plasmid DNA to bone marrow stromal cells. J Biomed Mater Res A 2007;81(2):493–504.
[29] Grandis JR, Drenning SD, Chakraborty A, Zhou MY, Zeng Q, Pitt AS, et al. Requirement of Stat3 but not Stat1 activation for epidermal growth factor receptor- mediated cell growth In vitro. J Clin Invest 1998;102(7):1385–92.
[30] Mora LB, Buettner R, Seigne J, Diaz J, Ahmad N, Garcia R, et al. Constitutive activation of Stat3 in human prostate tumors and cell lines: direct inhibition of Stat3 signaling induces apoptosis of prostate cancer cells. Cancer Res 2002;62(22):6659–66.
[31] Wang W, Edington HD, Rao UN, Jukic DM, Wang H, Shipe-Spotloe JM, et al. STAT3 as a biomarker of progression in atypical nevi of patients with melanoma: dose-response effects of systemic IFNalpha therapy. J Invest Dermatol 2008;128(8):1997–2002.
[32] Darnell JE. Validating Stat3 in cancer therapy. Nat Med 2005;11(6):595–6.
[33] Al Zaid Siddiquee K, Turkson J. STAT3 as a target for inducing apoptosis in solid and hematological tumors. Cell Res 2008;18(2):254–67.
[34] Xiong H, Zhang ZG, Tian XQ, Sun DF, Liang QC, Zhang YJ, et al. Inhibition of JAK1, 2/STAT3 signaling induces apoptosis, cell cycle arrest, and reduces tumor cell invasion in colorectal cancer cells. Neoplasia 2008;10(3):287–97.
[35] Sparano JA, Moulder S, Kazi A, Coppola D, Negassa A, Vahdat L, et al. Phase II trial of tipifarnib plus neoadjuvant doxorubicin-cyclophosphamide in patients with clinical stage IIB-IIIC breast cancer. Clin Cancer Res 2009;15(8):2942–8.
[36] Graness A, Poli V, Goppelt-Struebe M. STAT3-independent inhibition of lysophosphatidic acid-mediated upregulation of connective tissue growth factor (CTGF) by cucurbitacin I. Biochem Pharmacol 2006;72(1):32–41.
[37] Mackenzie GG, Queisser N, Wolfson ML, Fraga CG, Adamo AM, Oteiza PI. Curcumin induces cell-arrest and apoptosis in association with the inhibition of constitutively active NF-kappaB and STAT3 pathways in Hodgkin's lymphoma cells. Int J Cancer 2008;123(1):56–65.
[38] Dhillon N, Aggarwal BB, Newman RA, Wolff RA, Kunnumakkara AB, Abbruzzese JL, et al. Phase II trial of curcumin in patients with advanced pancreatic cancer. Clin Cancer Res 2008;14(14):4491–9.
[39] Gilmore IR, Fox SP, Hollins AJ, Akhtar S. Delivery strategies for siRNA-mediated gene silencing. Curr Drug Deliv 2006;3(2):145–55.
[40] Zhou W, Grandis JR, Wells A. STAT3 is required but not sufficient for EGF receptor-mediated migration and invasion of human prostate carcinoma cell lines. Br J Cancer 2006;95(2):164–71.
[41] Niu G, Shain KH, Huang M, Ravi R, Bedi A, Dalton WS, et al. Overexpression of a dominant-negative signal transducer and activator of transcription 3 variant in tumor cells leads to production of soluble factors that induce apoptosis and cell cycle arrest. Cancer Res 2001;61(8):3276–80.
[42] Kim SH, Jeong JH, Lee SH, Kim SW, Park TG. PEG conjugated VEGF siRNA for anti-angiogenic gene therapy. J Control Release 2006;116(2):123–9.
[43] Kim SH, Jeong JH, Lee SH, Kim SW, Park TG. Local and systemic delivery of VEGF siRNA using polyelectrolyte complex micelles for effective treatment of cancer. J Control Release 2008;129(2):107–16.
[44] Hsiao YW, Liao KW, Chung TF, Liu CH, Hsu CD, Chu RM. Interactions of host IL-6 and IFN-gamma and cancer-derived TGF-beta1 on MHC molecule expression during tumor spontaneous regression. Cancer Immunol Immunother 2008;57(7):1091–104.
[45] Rakemann T, Niehof M, Kubicka S, Fischer M, Manns MP, Rose-John S, et al. The designer cytokine hyper-interleukin-6 is a potent activator of STAT3-dependent gene transcription in vivo and in vitro. J Biol Chem 1999;274(3):1257–66.
[46] Haan S, Keller JF, Behrmann I, Heinrich PC, Haan C. Multiple reasons for an inefficient STAT1 response upon IL-6-type cytokine stimulation. Cell Signal 2005;17(12):1542–50.
[47] Costa-Pereira AP, Tininini S, Strobl B, Alonzi T, Schlaak JF, Is'harc H, et al. Mutational switch of an IL-6 response to an interferon-gamma-like response. Proc Natl Acad Sci U S A 2002;99(12):8043–7.
[48] Kakuta S, Tagawa Y, Shibata S, Nanno M, Iwakura Y. Inhibition of B16 melanoma experimental metastasis by interferon-gamma through direct inhibition of cell proliferation and activation of antitumour host mechanisms. Immunology 2002;105(1):92–100.
[49] Costanzo C, Piacentini G, Vicentini L, Armenante F, Mazzi P, Savio C, et al. Cell-specific differences in the regulation of IL-6 expression by PMA. Biochem Biophys Res Commun 1999;260(3):577–81.
[50] Libermann TA, Baltimore D. Activation of interleukin-6 gene expression through the NF-kappa B transcription factor. Mol Cell Biol 1990;10(5):2327–34.
[51] Kortylewski M, Kujawski M, Herrmann A, Yang C, Wang L, Liu Y, et al. Toll-like receptor 9 activation of signal transducer and activator of transcription 3 constrains its agonist-based immunotherapy. Cancer Res 2009;69(6):2497–505.
[52] Nishinakamura H, Minoda Y, Saeki K, Koga K, Takaesu G, Onodera M, et al. An RNA-binding protein alphaCP-1 is involved in the STAT3-mediated suppression of NF-kappaB transcriptional activity. Int Immunol 2007;19(5):609–19.
[53] Wang T, Niu G, Kortylewski M, Burdelya L, Shain K, Zhang S, et al. Regulation of the innate and adaptive immune responses by Stat-3 signaling in tumor cells. Nat Med 2004;10(1):48–54.
[54] Yu Z, Zhang W, Kone BC. Signal transducers and activators of transcription 3 (STAT3) inhibits transcription of the inducible nitric oxide synthase gene by interacting with nuclear factor kappaB. Biochem J 2002;367(Pt 1):97–105.
[55] Yang J, Stark GR. Roles of unphosphorylated STATs in signaling. Cell Res 2008;18(4):443–51.
[56] Chen Z, Han ZC. STAT3: a critical transcription activator in angiogenesis. Med Res Rev 2008;28(2):185–200.
[57] Ghosh S, Maity P. Augmented antitumor effects of combination therapy with VEGF antibody and cisplatin on murine B16F10 melanoma cells. Int Immunopharmacol 2007;7(13):1598–608.
[58] Niu G, Heller R, Catlett-Falcone R, Coppola D, Jaroszeski M, Dalton W, et al. Gene therapy with dominant-negative Stat3 suppresses growth of the murine melanoma B16 tumor in vivo. Cancer Res 1999;59(20):5059–63.